

## Developing the Optimal Geometry of the Trabecular Structure

ŘEHOUNEK Luboš<sup>1,a</sup> and JÍRA Aleš<sup>1,b</sup>

<sup>1</sup> Czech Technical University in Prague, Faculty of Civil Engineering, Department of Mechanics, Thákurova 7, 166 29, Prague, Czech Republic

<sup>a</sup>lubos.rehounek@fsv.cvut.cz, <sup>b</sup>jira@fsv.cvut.cz

**Keywords:** Dental Implant, Optimization, Porous, 3D Printing, SLM.

**Abstract.** This research deals with the problem of geometrical solutions of porous dental implants. The parameters associated with optimizing the geometry of the structure are usually overall porosity, cell size, wall thickness and mechanical parameters such as modulus of elasticity and hardness. We have developed a few variants of these structures according to the research of other authors. These structures were then assessed based on the difficulties associated with their manufacturing process and subsequently numerically analysed. The variant Diamond 30% relative density was evaluated as optimal among our current structures.

### Introduction

The long-term stability of implants is greatly influenced by their surface treatment. These treatments are usually done either by sand-blasting, acid-etching the surface or applying a plasmatic Ti coating onto the surface of the implant. The shortcomings of these methods is mainly their cost, demanding technological procedures and high surface stiffness of the implant [1].

With the advancement of additive manufacturing (AM) technologies, we are able to produce morphologically complex structures that resemble biological tissues, from both geometrical and mechanical standpoint [2]. These structures are usually 3D-printed using the Selective Laser Melting (SLM) or Selective Laser Sintering (SLS) technology and various metal powders (e.g. Ti-6Al-4V). The main goal of this work is to create and subsequently test and compare these structures.

The main reason behind creating new biostructures is increasing the implant success rates and decreasing the number of reoperations. This can be done by optimizing the structure so as to provide better stability during the early stages following implantation, where most failures occur due to the loss of stability [3]. The most common reasons for reoperation are mechanical release of the implant, infection and aseptic loss of stability or its dislocation [4].

**Trabecular Pore Size.** The process of optimizing the geometry of the trabecular structure is dependent on multiple factors. First, mechanical and biological factors come to mind. The latter are far more intriguing – no research to our knowledge has actually decisively determined the optimal size of the pores of the structure. There are, however, experiments that allude to a certain range of dimensions [5]. These dimensions should not, however, in our opinion, be taken as a definitive answer to the problem of pore size as they are performed under very special conditions that never truly resemble real live organisms. They should rather be taken as a recommendation towards other experiments to create more data.

The main properties to consider are overall porosity, wall/beam thickness, pore size and trabeculi orientation inside the 3D matrix. The problem of determining the optimal pore size

has been investigated before – as long ago as 1980 [6], authors have tried to come to a conclusion on optimal pore size. This particular research concluded that the greatest value of fixation strength was achieved using pore sizes in the range of 50-400  $\mu\text{m}$  (17 MPa at 8 weeks following the implantation). Other important research, too lengthy to describe in this short paper, can be found in the following references [7, 8].

Authors [5] investigated the effect of pore size of collagen-glycosaminoglycan scaffolds on proliferation of osteoblast MC3T3-E1 cells. Three time intervals were tested (24 hours, 48 hours, 7 days). The pore size that exhibited the greatest amount of cell proliferation across all time intervals is 325  $\mu\text{m}$  (62% of cells in contact with the structure) [5]. We consider this a viable starting information as there is not much research performed in this area.

The problem also gets more complicated as it is vital to observe *how* the bone material attaches to the structure (or the implant) and in what form. The process of healing and new bone formation is associated with cartilage formation and subsequent ossification and formation of osteons – the Haversian system [9]. During experiments, it is important to measure the volume of bone attached to the implant. This way, we can determine how well does a certain structure perform inside the living tissue as we need to distinguish between the bearing beams of the osteons and the low-mineralized fibrous tissue.

**Experiment.** We have previously conducted in-vivo tests on laboratory pigs with focus on bone contact percentage after 6 months following implantation (Fig. 1) [10]. This experiment is similar to the experiments carried out by authors mentioned above, however, it better and truly represents the conditions inside a living organism and the outcome we want to achieve. The pore size in this experiment was around 900  $\mu\text{m}$  and all specimens were 3D-printed using the Ti-6Al-4V metal powder alloy. We want to further investigate other, different structures with different pore sizes (Fig. 2), apply them onto real implants and redo the tests with pore sizes more corresponding to the findings presented by M. M. Ciara et al. [5].

It is important to note that the value of pore size of 325  $\mu\text{m}$  should not be considered final as it comes only from a single series of experiments and does not truly represent the nature of an in-vivo experiment. The authors of this work plan to take it as a base value and try to develop different structures and observe how they perform inside the aggressive surroundings of a living organism.

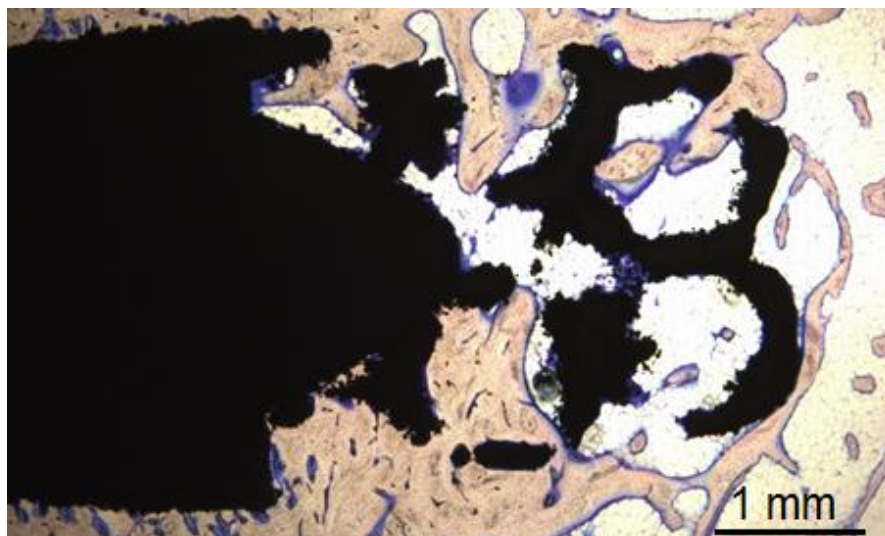


Fig.1 A longitudinal section of the trab. specimens extracted 6 months after implantation. White and light yellow color represents fibrous tissue, orange represents beams of newly formed bone tissue and black color represents the trabecular implant. In-vivo experiment performed at the Inst. of Animal Phys. and Gen., v. v. i., Liběchov

**Geometrical Solutions.** The main goal of this work is to create an optimal structure that will at the same time endure the mechanical loads and allow for the greatest amount of bone ingrowth and ongrowth. We have considered a total of 28 variants and decided to manufacture 3 variants shown below in Fig. 2. The pore sizes of all structures vary from 200  $\mu\text{m}$  to 450  $\mu\text{m}$ . The most promising structure seems to be the n.2 Diamond 30% relative density that has a pore size of approximately 340  $\mu\text{m}$  and does not exhibit any difficulties during manufacturing.

We have also created a few other basic models of other structures for comparison in numerical simulations. These structures will serve to give a better overview of possible variants and show possible flaws of design and places of stress concentrations (Fig. 3).

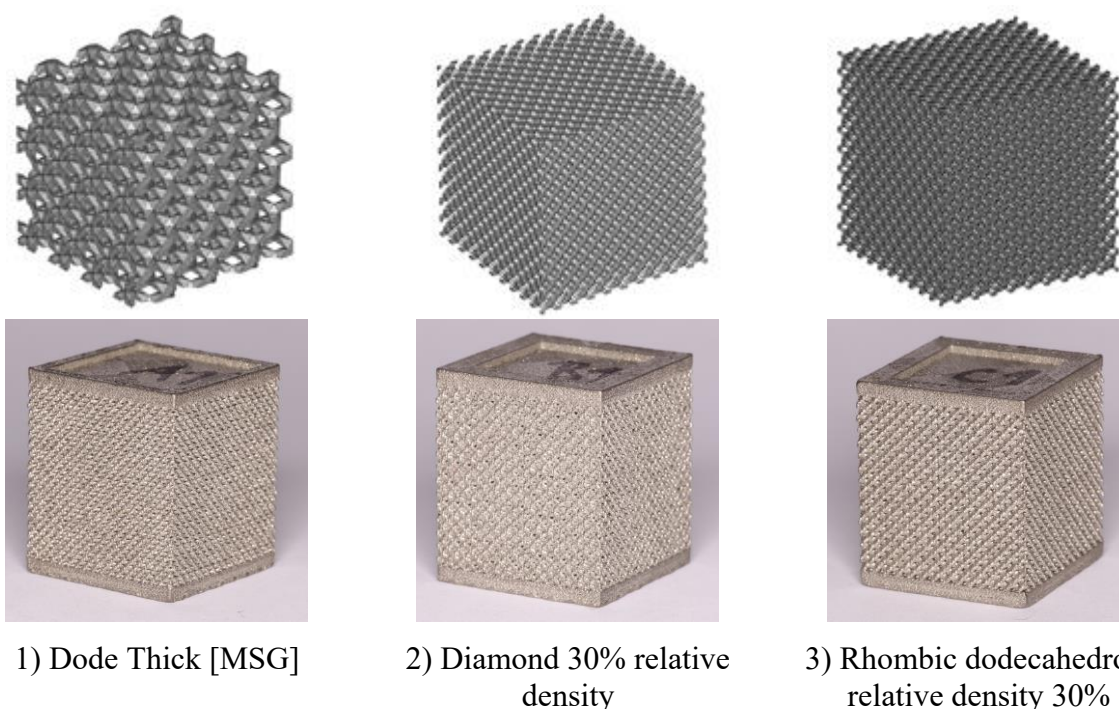


Fig.2 Upper row – figures of the .STL model files used to create the geometries of the final specimens. Bottom row – corresponding 3D-printed specimens for use in the uniaxial compression mechanical test. Used material is Ti-6Al-4V.

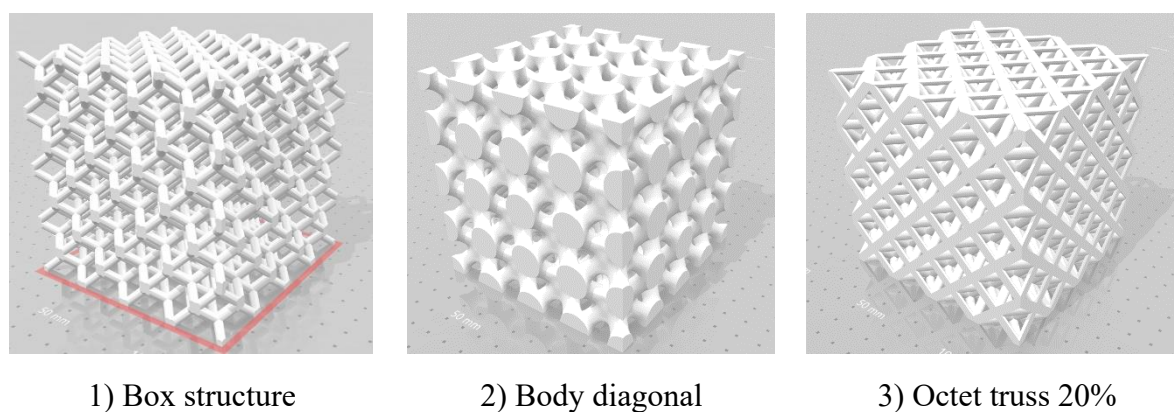


Fig.3 Other geometrical solutions of structures that will be used for comparison in the process of numerical simulations.

**Mechanical Tests.** We performed a series of macromechanical and micromechanical tests to determine the behavior of different trabecular structures. For this purpose, we performed uniaxial tensile and compression tests and nanoindentation test. The nanoindentation test proved the values of micromechanical properties dependent on the depth of the indent (the trend of reduced modulus  $E_r$  and hardness  $H_{it}$  is constant in the range of contact depth 470 nm or greater, see Fig. 4). The mean values of micromechanical properties of all specimens (not dependent on geometrical solution) are  $E_r = 118$  GPa and  $H_{it} = 5,187$  GPa. The micromechanical properties correspond with the values given by the manufacturer.

**Heat treatment.** The values of reduced modulus (Fig. 4 bottom) generally correspond with the values provided by other researchers [11], but the values of microhardness significantly vary. We have concluded that in the case of 3D-printed specimens, post-production heat treatment will play a significant role in the hardness of the final product. The values of hardness provided by our experiment (Fig. 4 top) are higher than most values provided by other research because they undergone a special annealing process that increased hardness significantly. Determining the right method of post-production heat treatment will be the next task in order to fully explore the capabilities of 3D-printed structures.

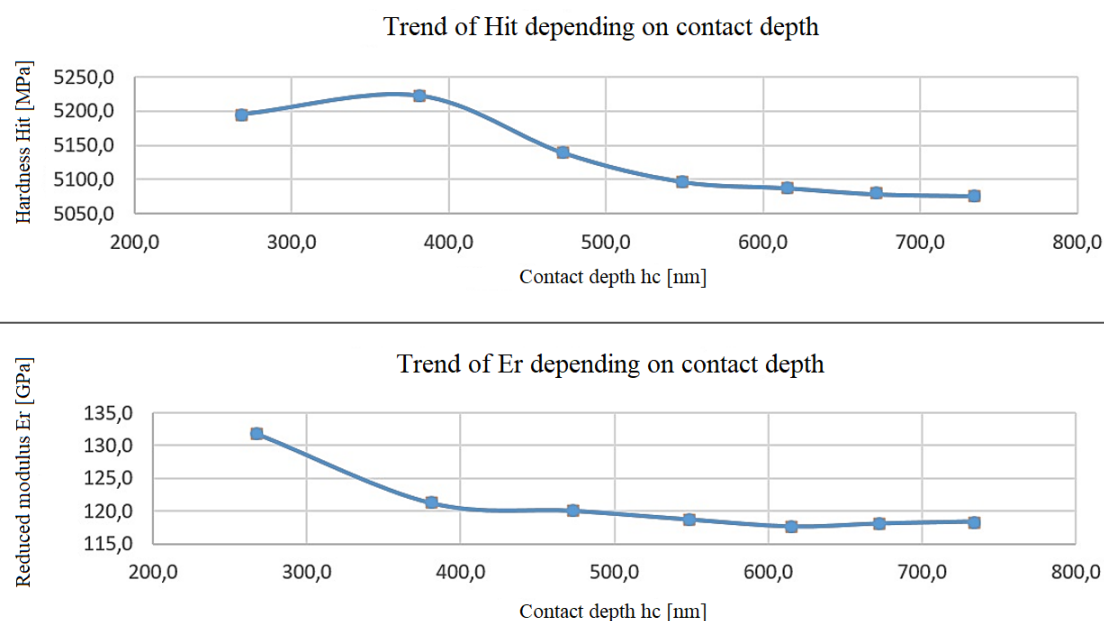


Fig.4 Two graphs showing the dependency of micromechanical properties on contact depth.

## Conclusions

Multiple geometrical solutions of the porous trabecular structure have been created and tested. The challenge to create a structure that is optimal in terms of new osteon formation inside the structure is met with mechanical challenges, namely values of modulus, ultimate strength of the structure and its ability to resist fragmentation.

We have evaluated the conditions for optimal bone ingrowth and decided to create our own specimens based on these rough values of pore sizes and observe which structure yields the best results.

Micromechanical tests proved the values of  $E_r$  and  $H_{it}$  of 3D-printed specimens (Fig. 4) are in accordance with the values of conventionally machined specimens. The macromechanical tests coupled together with a numerical model of the individual structures will show further insight into the behavior of the trabecular structures. The optimal structure also has to abide

by the conditions for osseointegration of the implant, which is yet another factor to account for when optimizing the geometry of the implant.

### Acknowledgment

The financial support by the Faculty of Civil Engineering, Czech Technical University in Prague (SGS project No. SGS17/168/OHK1/3T/11) and by the Technology Agency of the Czech Republic, project no. TJ01000328 is gratefully acknowledged.

### References

- [1] L. Řehounek, F. Denk, A. Jíra, Trabecular structures of dental implants formed by 3D printing and their mechanical properties, EAN 2016 - 54th International Conference on Experimental Stress Analysis, Czech Republic (2016).
- [2] L. Le Guéhennec et al., Surface treatments of titanium dental implants for rapid osseointegration, *Dental Materials* 23 (2007), 844-854.
- [3] R. B. Osman and M. V. Swain, A Critical Review of Dental Implant Materials with an Emphasis on Titanium versus Zirconia, *Materials* 8 (2015), 932-958.
- [4] R. Wauthle et al., Additively manufactured porous tantalum implants, *Acta Biomaterialia* 14 (2015), 217-225.
- [5] M. M. Ciara et al., The effect of mean pore size on cell attachment, proliferation and migration in collagen–glycosaminoglycan scaffolds for bone tissue engineering, *Biomaterials* 31 (2010), 461-466.
- [6] J. D. Bobyn et al., The optimum pore size for the fixation of porous-surfaced metal implants by the ingrowth of bone, *Clinical Orthopaedics and Related Research* 150 (1980), 263-270.
- [7] G. Campoli et al., Mechanical properties of open-cell metallic biomaterials manufactured using additive manufacturing, *Materials & Design* 49 (2013), 957-965.
- [8] S. A. Yavari, Bone regeneration performance of surface-treated porous titanium, *Biomaterials* 35 (2014), 6172-6181.
- [9] A. M. Phillips, Overview of the fracture healing cascade, *Injury* 36 (2005), 5-7.
- [10] L. Řehounek and A. Jíra, Numerical and Mechanical Analyses of a 3D-printed titanium trabecular dental implant, *Acta Polytechnica* 57 (2017), 218-228.
- [11] S. Q. Wu, Microstructural evolution and microhardness of a selective-laser-melted Ti–6Al–4V alloy after post heat treatments, *Journal of Alloys and Compounds* (2016), 643-652.

## The Chloride Ion Penetration Resistance of Fine Recycled Aggregate Concrete

SEFFLOVA Magdalena<sup>1,2,a</sup>

<sup>1</sup>CTU in Prague, University Centre of Energy Efficient Buildings, Trinecka 1024, 273 43, Bustehrad, The Czech Republic

<sup>2</sup>CTU in Prague, Faculty of Civil Engineering, Department of Building Structures, Thakurova 7, 160 00, Prague, The Czech Republic

<sup>a</sup>magdalena.sefflova@fsv.cvut.cz

**Keywords:** Chloride ion penetration, Fine recycled aggregate, Durability.

**Abstract.** This paper is focused on chloride ion penetration of fine recycled aggregate (FRA) concrete. The durability of FRA concrete is connected with doubts. A total four concrete mixtures were designed. The first concrete mixture was reference, only with natural aggregate. In other concrete mixtures, natural aggregate was replaced by FRA in varying replacement ratio. Chloride ion penetration resistance of FRA aggregate was tested. The test results showed that the use FRA in concrete influences chloride ion penetration of concrete.

### Introduction

The chloride ion penetration resistance is one of the most important durability concrete properties. Primarily the question of durability is very important for recycled aggregate concrete. The use coarse fraction of recycled aggregate is already accepted but with specific restrictions [1]. After literature review it is possible to say that many researchers obtained totally different results. One of many studies observed that chloride ion penetration of coarse recycled aggregate concrete is not significantly different from concrete without recycled aggregate [2]. Evangelista [3] showed contrary results. The chloride ion penetration resistance is reduced by adding of recycled aggregate in concrete mixtures.

The problem is with the use the FRA. A little researcher studies of FRA concrete durability were published. Therefore, this paper is focused on the chloride ion penetration of FRA concrete.

### Experimental Research Program

**Materials.** Portland cement CEM I 42.5 R, natural sand, water and the FRA were used in the experimental program. The FRA originated from crushed concrete waste. Concrete waste was crushed to fraction 32/64 mm in the recycling plant and to fraction 0/4 mm by jaw crusher in the laboratory. There were tested geometrical and physical properties of FRA. Testing results were comparison with natural sand. The test results of physical properties of aggregate are given in Tab. 1. The geometrical properties are given in Fig. 1.

Tab. 1 Physical properties of FRA and natural sand

Types of aggregate	Fraction [mm]	Density[kg/m <sup>3</sup> ]	Water absorption capacity [%]
FRA	0 – 4	2090	8,29
Natural sand	0 – 4	2600	2,00

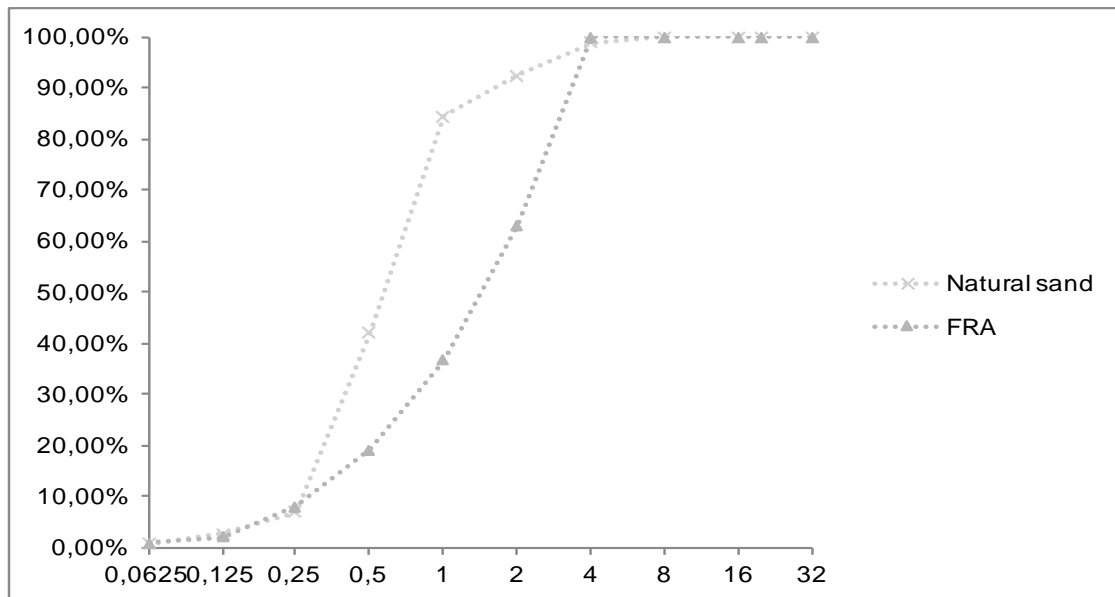


Fig. 1 Geometrical properties of natural sand and FRA

**Concrete mixtures.** A total four concrete mixtures were designed. All concrete mixtures were designated with same amount of cement and the same w/c ratio for clear comparison. The first concrete mixture was prepared only with natural sand (REF). In other mixtures, natural sand was replaced by FRA in varying replacement ratio (specifically 50 %, 60 % and 70 %). All concrete mixtures are given in Tab. 2.

Tab. 2 Concrete mixtures

Designation	REF	REC50	REC60	REC70
cement [kg/m <sup>3</sup> ]	486	486	486	486
water [kg/m <sup>3</sup> ]	243	243	243	243
natural sand [kg/m <sup>3</sup> ]	1458	729	583	438
FRA [kg/m <sup>3</sup> ]	0	729	875	1020

**Testing.** Beams of dimensions 40x40x160 mm were used for the testing. Chloride ion penetration was tested according to CSN 73 1326 [4]. The surface of concrete samples (40 x 160 mm) was plunged in 3 % NaCl solution. Concrete samples were exposed a total 100 freeze – thaw cycles. One freeze – thaw cycle took around 2 hours and was composed of

freezing on temperature  $-15\text{ }^{\circ}\text{C}$  (minimal duration 15 minutes) and thawing on temperature  $20\text{ }^{\circ}\text{C}$  (minimal duration 15 minutes). A pass was made at depth to grind the concrete samples into dust after each 25 cycles, which were then collected.

**Results.** Fig. 2 shows a concrete pass after 25, 50, 75 and 100 cycles. It is evident that concrete samples REC50 show the worse chloride ion penetration resistance. The concrete pass was almost  $1800\text{ g/m}^2$  after 100 cycles. The reference concrete samples show also poor chloride ion penetration resistance. The pass of reference concrete was  $1319\text{ g/m}^2$ . In comparison with this, the best chloride ion resistance showed concrete samples with 60 % replacement ratio. The pass of concrete REC60 was  $967\text{ g/m}^2$  after 100 cycles. Fig. 3 and Fig. 4 show concrete surface disruption after 100 CHLR cycles.

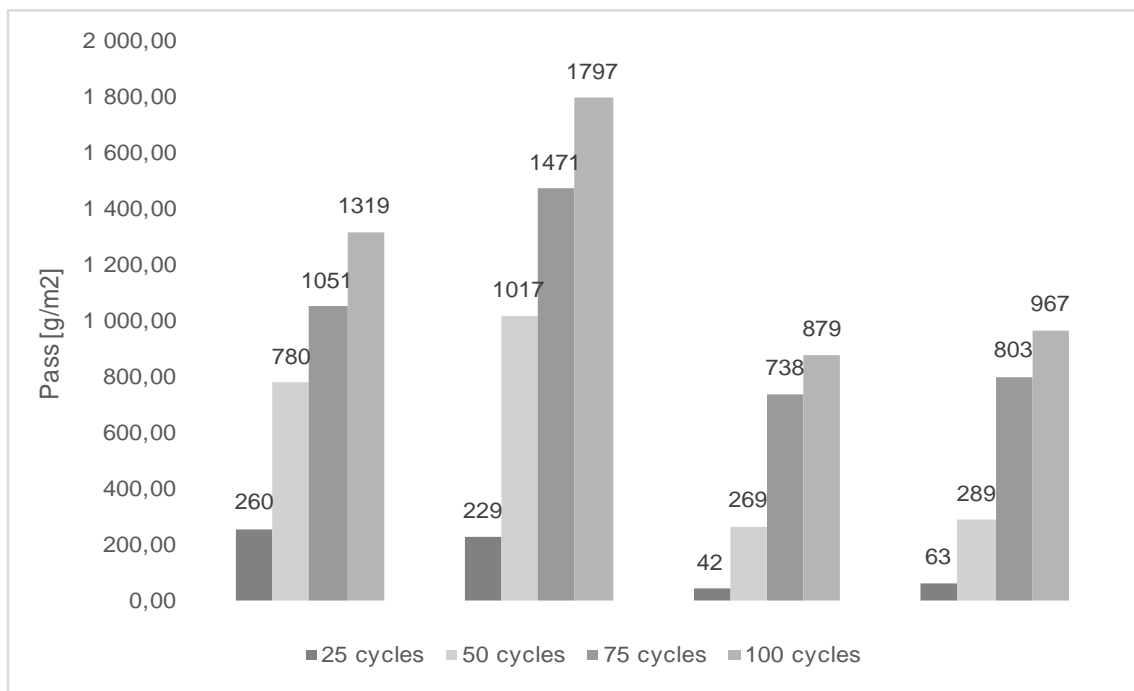


Fig. 2 Concrete pass after 25, 50, 75 and 100 CHLR cycles



Fig. 3 Concrete surface disruption after 100 CHLR cycles – REF concrete

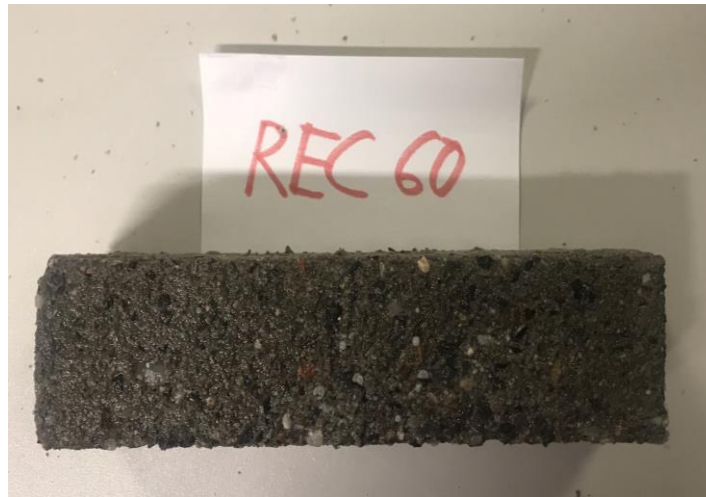


Fig. 4 Concrete surface disruption after 100 CHLR cycles – REC60 concrete

### Conclusions

In conclusion, it is possible to say that the use of the FRA in concrete as a partial replacement of natural sand influences chloride ion penetration of concrete. The test results are very satisfactory and confirm the assumption of the possible use of the FRA even with a higher replacement ratio. However, it is necessary to verify these results in future research.

### Acknowledgement

This work has been supported by the Ministry of Education, Youth and Sports within National Sustainability Programme I, project No. LO1605 – Energy efficient construction and demolition waste into building structures and by TH02030649 Environmental efficiency building waste into building structures and by SGS18/108/OHK1/2T/11 Environmental aspects of high performance cement composites and concrete with recycled aggregate including their durability and service life.

### References

- [1] CSN EN 206. Concrete – Specification, performance, production and conformity. Prague: Czech standards institute, 2014 (in Czech).
- [2] Gomes, M., 2009. Structural concrete with incorporation of coarse recycled concrete and ceramic aggregates: durability performance. *Materials and Structures*, 42 (5), 2009, pp. 663 – 675.
- [3] Evangelista L., 2010. Durability performance of concrete made with fine recycled concrete aggregates. *Cement and Concrete Composites*, 32 (1), 2010, pp. 9 – 14.
- [4] CSN 73 1226. Determination of cement concrete surface resistance to water and chemical defrosting materials. Prague: Czech standards institute, 1984 (in Czech)